Electronic Supplementary Material (ESI) for Sustainable Energy & Fuels.

Supplementary Information

Title: Mitigating voltage losses in photoelectrochemical cell scale-up

Authors: Fatwa F. Abdi[1*], Ronald Ramiro Gutierrez Perez[2], Sophia Haussener[2]

Affiliations:

[1] Institute for Solar Fuels, Helmholtz-Zentrum Berlin für Materialien und Energie GmbH, Hahn-Meitner-Platz 1, Berlin 14109, Germany

[2] Laboratory of Renewable Energy Science and Engineering, Institute of Mechanical Engineering, École Polytechnique Fédérale de Lausanne, 1015 Lausanne, Switzerland

[*] correspondence: fatwa.abdi@helmholtz-berlin.de

Supplementary Note 1

These are the steady-state governing transport (Nernst-Planck equation) and conservation equations of the ionic species, considering charge neutrality:

$$-\nabla . N_i + R_i = 0 \tag{S1}$$

$$N_i = -D_i \nabla c_i - \frac{z_i D_i}{RT} F c_i \nabla \phi_\mathrm{l} + c_i u \tag{S2}$$

N_i is the molar flux vector, R_i is the reaction source term, D_i is diffusivity, c_i is the concentration, and z_i is the charge of species i. u is the electrolyte velocity vector, F is Faraday's constant and ϕ_l is the electrolyte potential. The above equations apply for H^+, K^+, HPO_4^{2-} and $H_2PO_4^-$ in our study. Local equilibrium of buffer species (i.e., H^+, HPO_4^{2-} and $H_2PO_4^-$) was also assumed. For the dissolved neutral species (i.e., H_2 and O_2), equation S2 is simplified to the diffusion-advection equation where $z_i = 0$. The velocity term was determined by solving the mass and momentum (Navier-Stokes equation) conservation equations under laminar flow condition.

$$\nabla . u = 0 \tag{S3}$$

$$\rho u . \nabla u = -\nabla p + \mu \nabla^2 u + \rho g \tag{S4}$$

ρ is the density, p is the pressure, μ is the viscosity and g is gravity. At the electrode surface, mass fluxes were determined by the local current density (i_loc) and the stoichiometry coefficients (ν_i) of the redox equilibrium reaction.

$$\nu_{\mathrm{Ox}}Ox + ne^{-} \rightleftharpoons \nu_{\mathrm{Red}}Red \tag{S5}$$

$$R_i = \frac{-\nu_i i_{\mathrm{loc}}}{nF} \tag{S6}$$

The stoichiometry coefficients for H^+, H_2 and O_2 are −4, 2 and −1, respectively, when the number of electrons (n) is 4. The local electrode current density (i_{loc}) was determined by Butler-Volmer equation.

$$i_{\mathrm{loc}} = j_0 \left\{ exp\left(\frac{\alpha_{\mathrm{a}} F\eta}{RT}\right) - exp\left(\frac{-\alpha_{\mathrm{c}} F\eta}{RT}\right) \right\} \tag{S7}$$

j_0, α_a and α_c are exchange current density, anodic and cathodic transfer coefficient, respectively. The overpotential (η) for the anode and cathode was determined by:

$$\eta_{\mathrm{anode}} = \phi_{\mathrm{s}} - \phi_{\mathrm{l}} - 1.23 + \frac{RT}{2F}\ln\frac{c_{\mathrm{H^+,bulk}}}{c_{\mathrm{H^+}}} \tag{S8}$$

$$\eta_{\mathrm{cathode}} = \phi_{\mathrm{s}} - \phi_{\mathrm{l}} - 0 + \frac{RT}{2F}\ln\frac{c_{\mathrm{H^+,bulk}}}{c_{\mathrm{H^+}}} \tag{S9}$$

ϕ_{s} is the electrode potential. The Ohm's law governs the transport of charge in the electrode, and Nernst-Planck equation determines the charge transport in the electrolyte.

$$i_{\mathrm{s}} = -\sigma_s \nabla \phi_{\mathrm{s}} \tag{S10}$$

$$i_{\mathrm{l}} = F \sum_i z_i N_i \tag{S11}$$

$$i_l = -i_s = \sum i_{loc} \tag{S12}$$

i_l and i_s are the current density in the electrolyte and electrode, respectively, and σ_s is the electrode conductivity (see manuscript for further descriptions of σ_s). Steady-state solutions of all the governing and conservation equations were obtained using the MUMPS solver, which is a direct method based on lower-upper (LU) factorization (matrix triangulation), and the following dependent variables: p, u, ϕ_l, ϕ_s, c_{H^+}, $c_{HPO_4^{2-}}$, $c_{H_2PO_4^-}$, c_{O_2}, c_{H_2}.

Table S1. Table of baseline parameters used in the simulations. Unless specifically mentioned in the manuscript text or figure captions, the parameters here were used.

	Parameter	**Value**	**Ref.**
Electrolyte	Initial H^+ concentration, $c_{H^+,i}$	10^{-7} M (pH = 7)	
	Initial HPO_4^{2-} concentration, $c_{HPO_4^{2-},i}$	1.2 M	
	Initial $H_2PO_4^-$ concentration, $c_{H_2PO_4^-,i}$	0.8 M	
	Initial dissolved O_2 concentration, $c_{O_2,i}$	0 M	
	Initial dissolved H_2 concentration, $c_{H_2,i}$	0 M	
	Diffusivity of H^+, D_{H^+}	9.3×10^{-9} m^2/s	S1-2
	Diffusivity of K^+, D_{K^+}	1.96×10^{-9} m^2/s	S1-2
	Diffusivity of HPO_4^{2-}, $D_{HPO_4^{2-}}$	0.69×10^{-9} m^2/s	S1
	Diffusivity of $H_2PO_4^-$, $D_{H_2PO_4^-}$	0.85×10^{-9} m^2/s	S1
	Buffer equilibrium constant, K_{eq}	1.5×10^{-4} mol/m^3	S3
	Diffusivity of O_2, D_{O_2}	2.4×10^{-9} m^2/s	S1
	Diffusivity of H_2, D_{H_2}	5×10^{-9} m^2/s	S1
	Inlet velocity, v_{in}	0.27 cm/s	
	Inlet entrance length, L_{entr}	0.01 m	
	Outlet pressure, p_{out}	10^5 Pa	
	Dynamic viscosity, μ	0.89 mPa s	S1
	Density, ρ	998.5 kg/m^3	S1
	Temperature	300 K	
Electrode	HER exchange current density, $i_{0,HER}$	10 A/m^2	S4-5
	HER anodic transfer coefficient, $\alpha_{a,HER}$	0.5	
	HER cathodic transfer coefficient, $\alpha_{c,HER}$	0.5	
	OER exchange current density, $i_{0,OER}$	10^{-4} A/m^2	S4,S6-8
	OER anodic transfer coefficient, $\alpha_{a,OER}$	1.9	
	OER cathodic transfer coefficient, $\alpha_{c,OER}$	0.1	
	Electrode conductivity, σ_{el}	10^5 S/m	
	Applied average current density, $j_{app,s}$	10 mA/cm^2	
Geometry	Cell height, h_{cell}	10 cm	
	Cell width, w_{cell}	3 cm	
	Electrode height, h_{el}	8 cm	
	Electrode thickness, simulated, d_{el}	1 mm	
	Electrode thickness, real, $d_{el,0}$	0.5 µm	

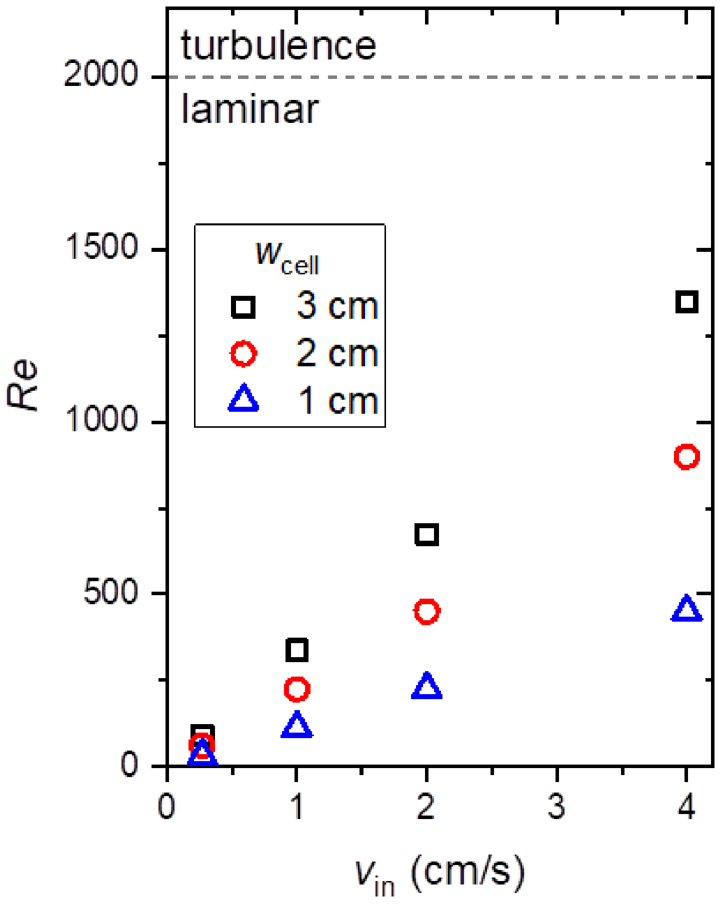

Figure S1. Reynolds number (*Re*) for the various cell widths (w_{cell}) and inlet velocities (v_{in}) investigated in this study. For all combinations, *Re* remains well below the laminar-turbulence transition value.

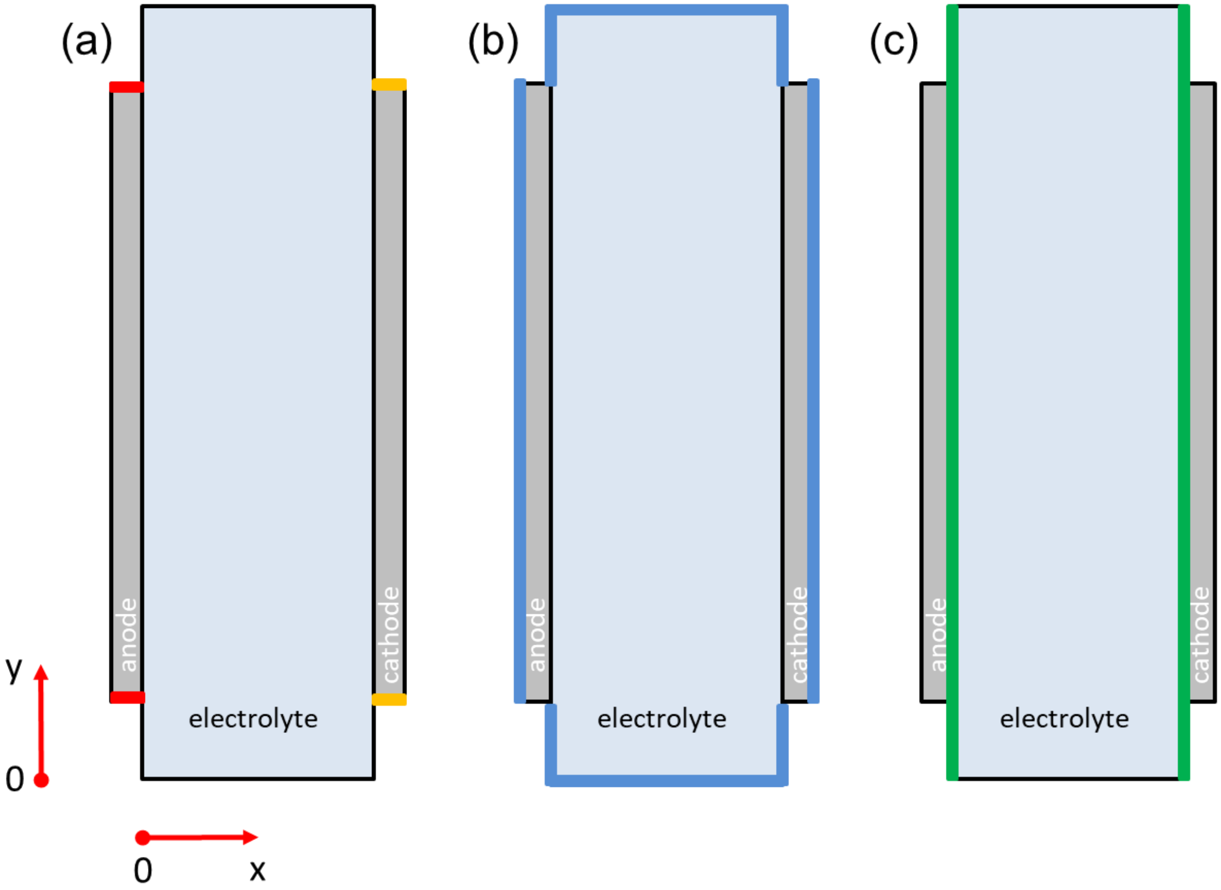

Figure S2. Schematic of the cell indicating edges where several boundary conditions were applied: **(a)** average current density at the anode's electrical contact (red) and ground at the cathode's electrical contact (orange), **(b)** insulation, $-n.i_s = 0$ (blue edges), and **(c)** no flux, $-n.J_i = 0$ (green edges).

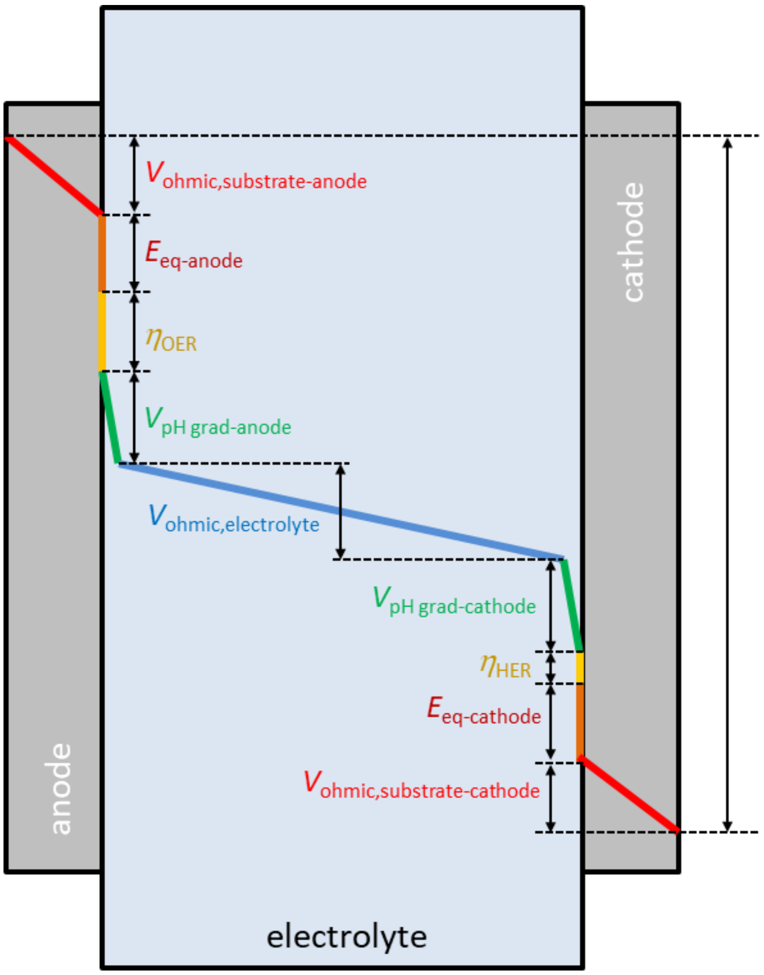

Figure S3. Schematic illustration of potential distribution within the cell, which constitutes the total cell voltage (V_{cell}). $V_{\text{ohmic,substrate-anode}}$ = substrate ohmic loss at the anode, $V_{\text{ohmic,substrate-cathode}}$ = substrate ohmic loss at the cathode, $E_{\text{eq-anode}}$ = thermodynamic equilibrium potential for the reaction at the anode surface, $E_{\text{eq-cathode}}$ = thermodynamic equilibrium potential for the reaction at the cathode surface, η_{OER} = kinetic overpotential for the oxygen evolution reaction, η_{HER} = kinetic overpotential for the hydrogen evolution reaction, $V_{\text{pH grad-anode}}$ = Nernstian loss due to pH gradients at the surface of the anode, $V_{\text{pH grad-cathode}}$ = Nernstian loss due to pH gradients at the surface of the cathode, $V_{\text{ohmic,electrolyte}}$ = electrolyte ohmic loss.

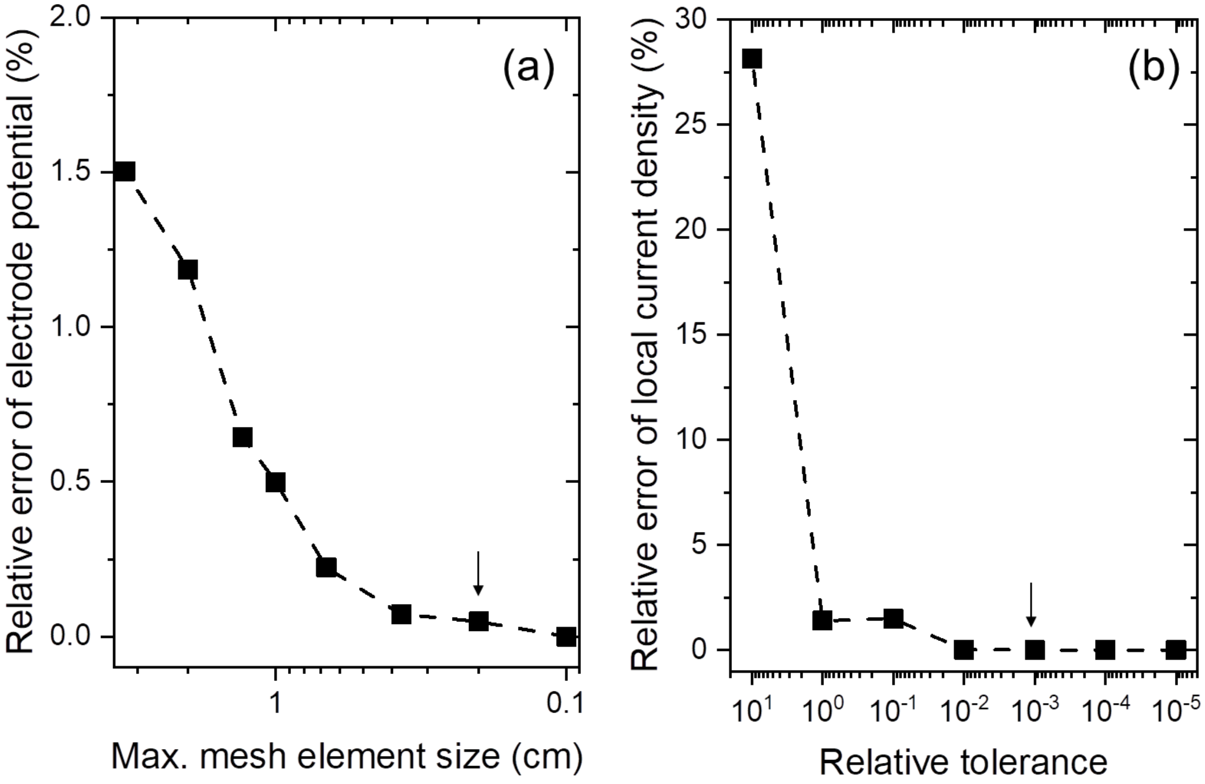

Figure S4. Relative error of **(a)** average electrode potential for varying maximum mesh element size and **(b)** average local current density for varying relative tolerance. The black arrows show the chosen mesh size and relative tolerance for our simulations.

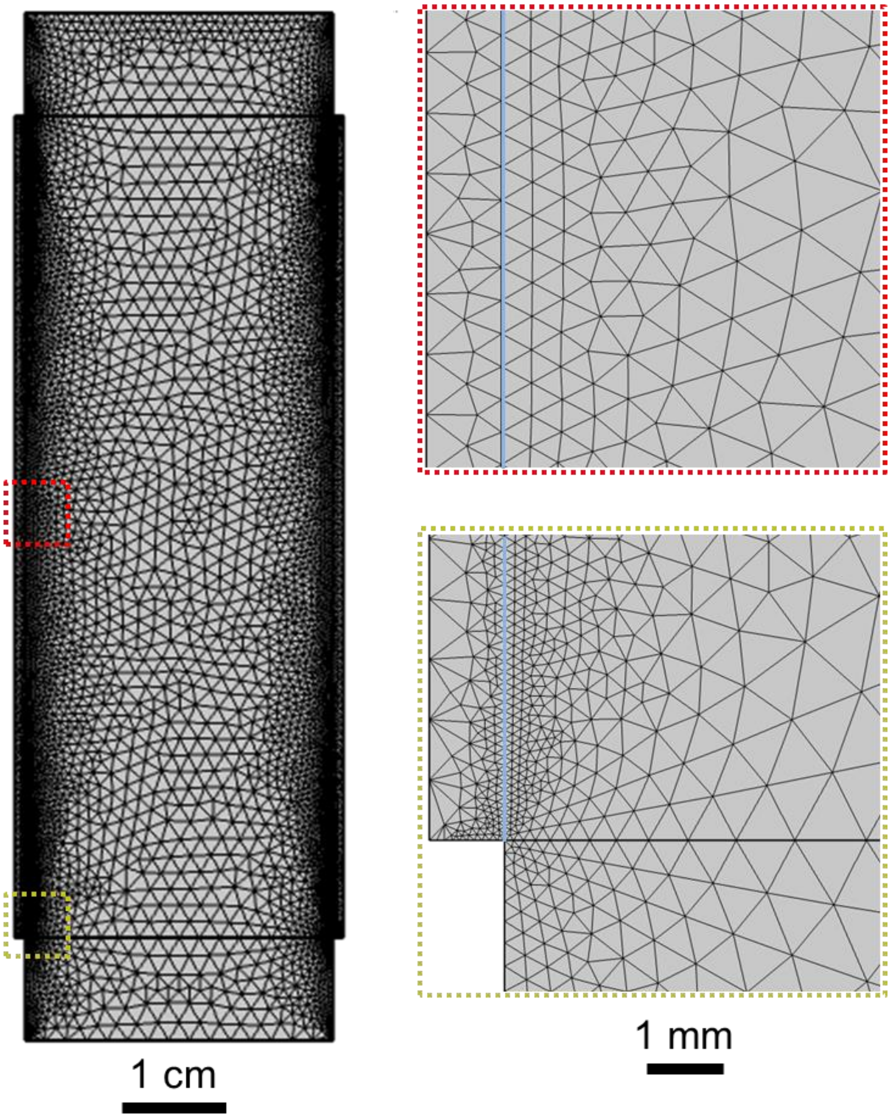

Figure S5. Optimized mesh configuration used in this study. Magnifications of area close to the center of the electrodes (red) and at the edges of the electrode (yellow) are also shown. The vertical blue line in these magnified figures identifies the electrode-electrolyte interface.

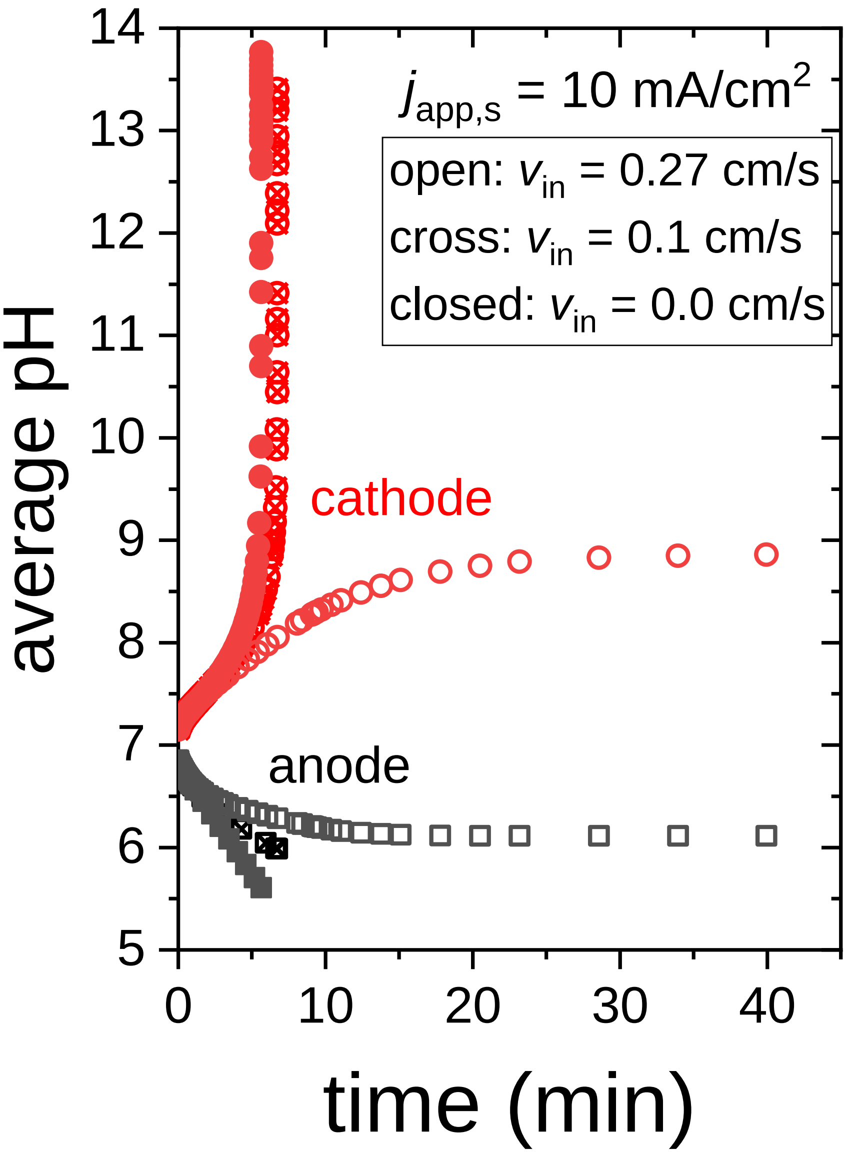

Figure S6. Time-dependent average pH at the surface of the anode (black) and cathode (red) for inlet velocity (v_{in}) of 0.0 and 0.27 cm/s. The average current density at the surface of the electrodes ($j_{app,s}$) is 10 mA/cm^2.

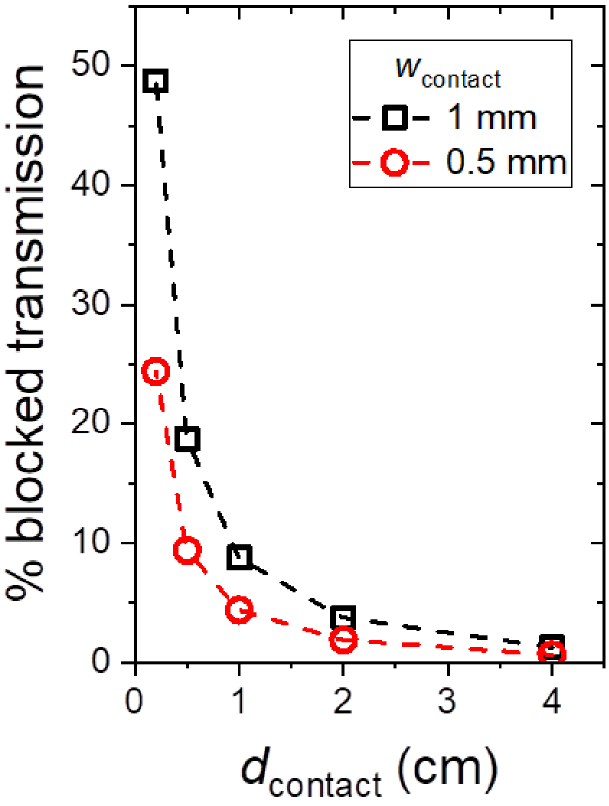

Figure S7. Percentage of transmitted light that are blocked by the metallic lines for various contact widths (w_{contact}) and spacing between the metallic lines (d_{contact}). Note that a decrease of w_{contact} results in higher resistive loss within the metallic lines; for a silver line with a thickness of 2 μm, an average length of 2 cm and d_{contact} of 1 cm, the voltage loss along the line is 18 and 36 mV for w_{contact} of 1 and 0.5 mm, respectively ($j_{\text{app,s}}$ = 10 mA/cm^2).

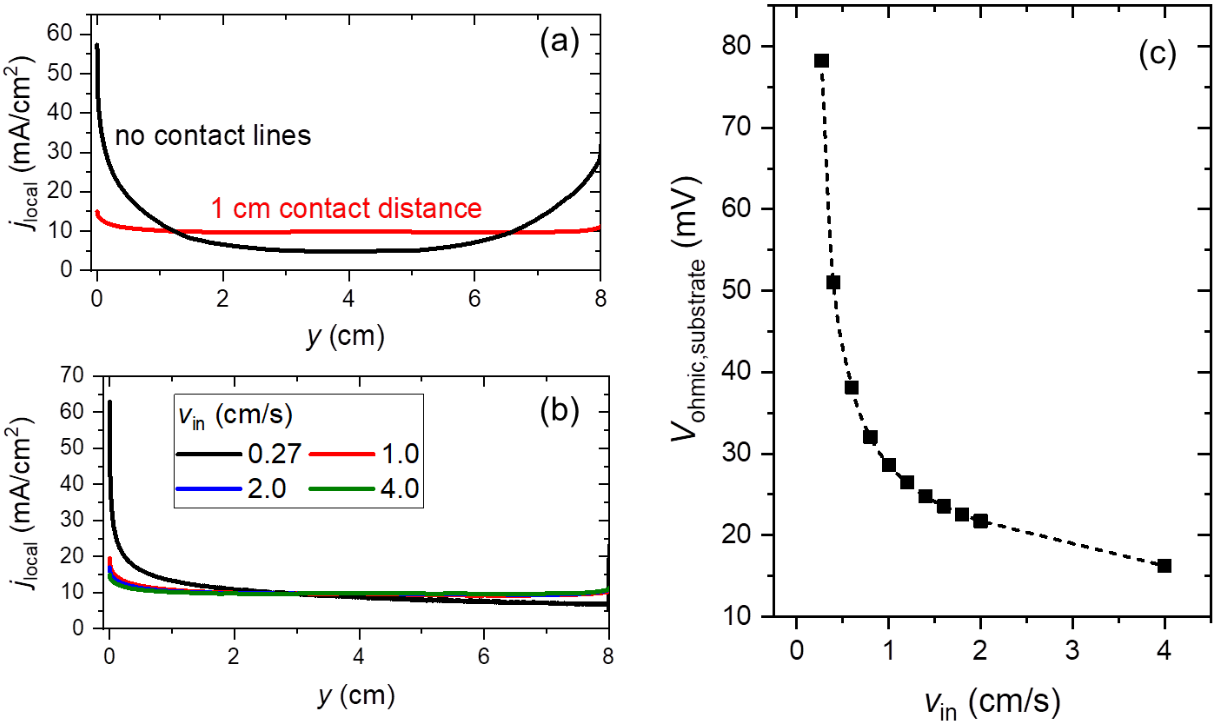

Figure S8. Local current density distribution at the surface of the electrode (cathode) **(a)** with and without 1 cm Ni lines (v_{in} = 4 cm/s) and **(b)** for various inlet velocities ($d_{contact}$ = 1 cm). **(c)** Substrate ohmic loss with increasing inlet velocity. The electrodes have metallic lines with spacing of 1 cm. The electrolyte is 2 M KP_i buffer (pH 7). $j_{app,s}$ = 10 mA/cm^2, h_{el} = 8 cm, h_{cell} = 10 cm, and w_{cell} = 3 cm.

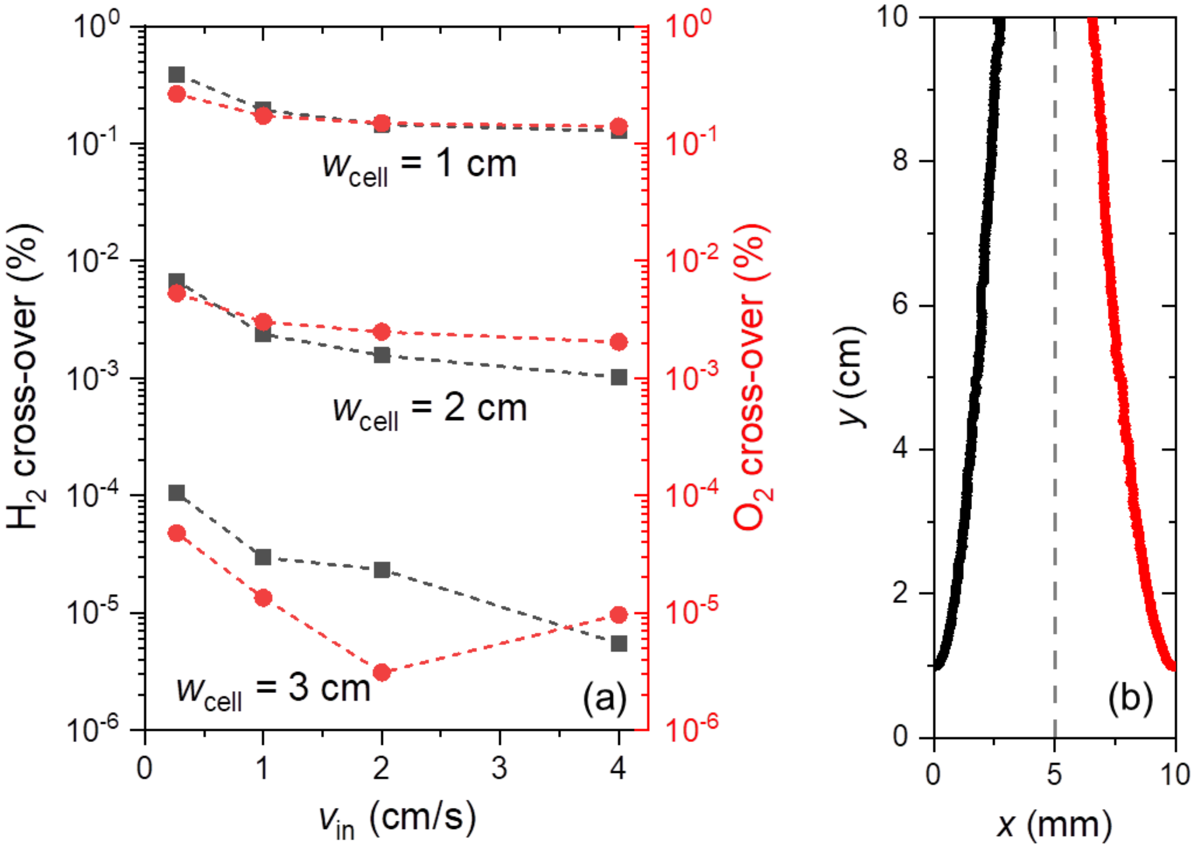

Figure S9. (a) Product crossover as a function of inlet velocity for various cell widths. **(b)** Concentration contour for O_2 (black) and H_2 (red) where $c_i = 0.01 \times c_i|_{x=\text{surface},y=\text{outlet}}$. The electrolyte is 2 M KP_i buffer (pH 7). Faraday efficiency of 100% is assumed. $j_{app,s}$ = 10 mA/cm^2, h_{el} = 8 cm, and h_{cell} = 10 cm.

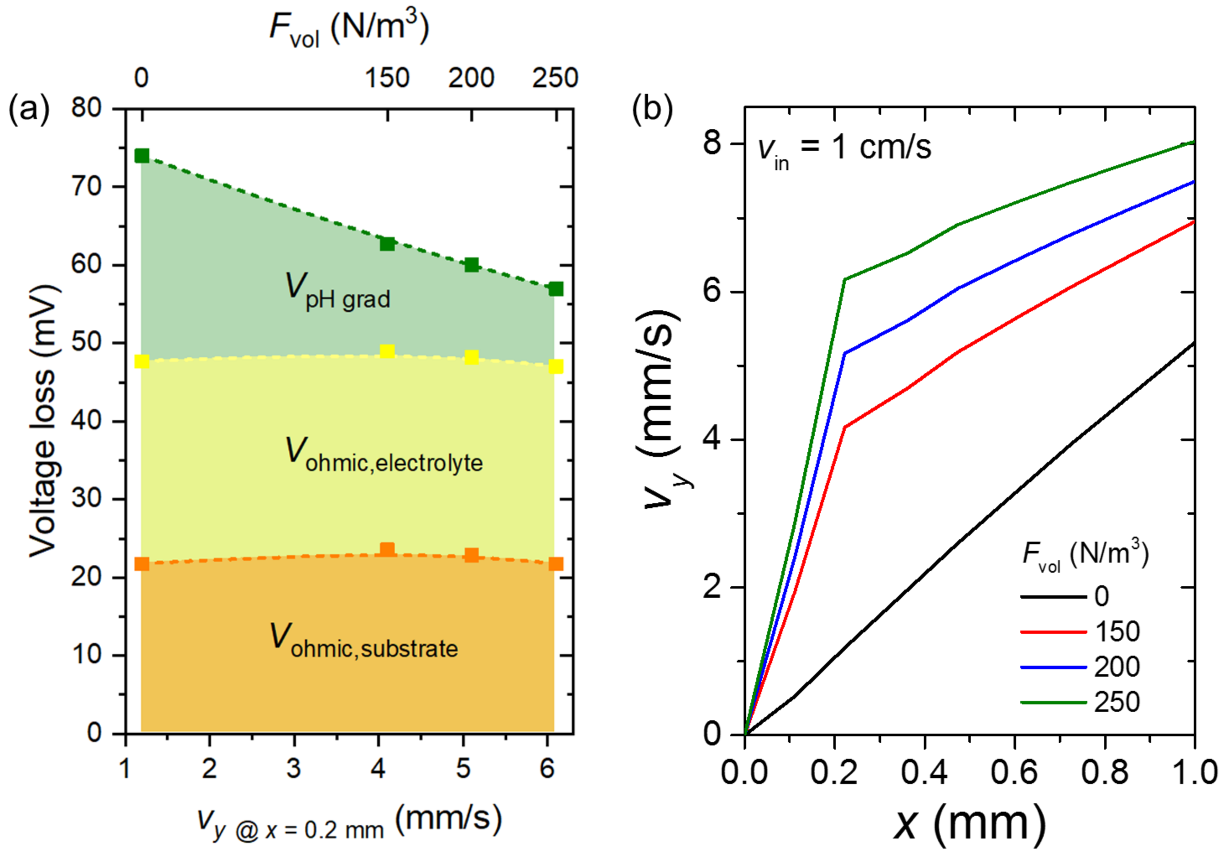

Figure S10. (a) Contribution of the electrolyte ohmic loss ($V_{ohmic,electrolyte}$), the pH gradient loss ($V_{pH\ grad}$), and the substrate ohmic loss ($V_{ohmic,substrate}$) as a function of the electrolyte velocity close to the electrodes (see bottom *x*-axis), as obtained by including the respective volume force (F_{vol}, see top *x*-axis) to simulate bubble-induced convection. The electrolyte velocity profiles close to the electrodes are shown in **(b)**. The electrolyte is 2 M KP_i buffer (pH 7). $j_{app,s}$ = 10 mA/cm^2, v_{in} = 1 cm/s, h_{cell} = 10 cm, h_{el} = 8 cm, $d_{contact}$ = 1 cm, and w_{cell} = 1 cm.

Reference

S1. W. M. Haynes, *CRC Handbook of Chemistry and Physics, 97th ed.*, CRC Press, Boca Raton, FL, 2016.

S2. U.S. Geological Survey thermodynamic database "*phreeqc.dat*".

S3. A. A. Green, *J. Am. Chem. Soc.*, **1933**, *55*, 2331-2336

S4. S. Haussener, C. Xiang, J. M. Spurgeon, S. Ardo, N. S. Lewis and A. Z. Weber, *Energy Environ. Sci.*, **2012**, *5*, 9922-9935.

S5. S. Trasatti, *J. Electroanal. Chem. Interf. Electrochem.*, **1972**, *39*, 163-184.

S6. G. Lodi, E. Sivieri, A. De Battisti and S. Trasatti, *J. Appl. Electrochem.*, **1978**, *8*, 135-143.

S7. M. G. Walter, E. L. Warren, J. R. McKone, S. W. Boettcher, Q. Mi, E. A. Santori and N. S. Lewis, *Chem. Rev.*, **2010**, *110*, 6446-6473.

S8. K. Kinoshita, *Electrochemical oxygen technology*, John Wiley & Sons, 1992.